Research Article

PHASE DIAGRAM, THERMODYNAMIC ANALYSIS AND INTERFACIAL STUDIES ON SOLID DISPERSIONS OF PHENOTHIAZINE-B. NAPHTHOL DRUG SYSTEM

Shekhar H. and Kumar Manoj
Department of Chemistry, V.K.S. University, Ara-802301, India
*Author for Correspondence

ABSTRACT

The study of solid liquid dispersions of binary drug system has been very useful in providing the significant enhanced pharmaceutical properties as compared to the parent drug. The present communication includes the thermodynamic and interfacial investigation of phenothiazine (PT) and β Naphthol (βN) binary eutectic and non-eutectic drug dispersion. Simple eutectic dispersion was observed at 0.763 mole fraction of βN at melting temperature 110°C. Partial and Integral thermodynamic quantities such as, excess Gibbs energy (g^E), excess enthalpy (h^E), excess entropy (s^E) of eutectic and non-eutectic mixtures were also calculated using activity coefficient data. The value of excess Gibbs free energy indicates positive deviation from ideal behaviour which refers stronger association between like molecules during formation of binary mix. However, the negative value of mixing function, Gibbs free energy of mixing (ΔG^M) suggests the mixing for eutectic and non-eutectic is spontaneous. The interfacial properties such as entropy of fusion per unit volume (ΔS_V), interfacial energy (σ), roughness parameter (α), grain boundary energy of parent components, eutectics and non-eutectics have been studied using enthalpy of fusion data. Gibbs-Thomson coefficient evaluated by numerical method is also very helpful to compute the interfacial energy. The size of critical nucleus at different undercoolings has been found in nanoscale, which may lead a big challenge in pharmaceutical world. The value of $\alpha > 2$, suggests the irregular and faceted growth proceeds in binary alloys.

Keywords: Phase Diagram, Thermodynamic and Mixing Functions, Thermal Stability, Critical Radius, Interfacial Energy and Microstructure

INTRODUCTION

Phenothiazine is a bioactive heterocyclic compound having pharmaceutical importance and shows various biological activities such as antifungal, antibacterial, anti-tubercular, anti-inflammatory, anti-schizophrenic, antipsychotic, antihistaminic, etc (Domínguez *et al.,* 1997, Guerrero *et al.,* 2008). The tricyclic compound has two active sites makes it a giant pharmaceutical molecule. During last few years the solid dispersion of binary pharmaceutical systems are being used as model system for studying the rapid growth of nano particles and microstructures which are very important parameters in controlling the final physical, chemical and medicinal properties of solid dispersion (Attila *et al.,* 2010, Bai *et al.,* 2006, Yu *et al.,* 2003). Others parameters of these dispersions can also be understood to a great extent with the help of kinetic, thermodynamic and interfacial investigation. Phenothiazines have gained much significant importance in the area of pharmaceutical applications. Other side β naphthol nucleus constitutes an important part of the vitamin B_{12}. These compounds are an important class of heterocyclic compounds which show diverse types of biological and pharmacological properties. Several derivatives of β naphthol have been reported as antagonists, prostaglandin D2, angotencin II receptors, dopamine β-hydroxylase inhibitors and inhibitors for endothelial cell growth. In addition, β naphthol derivatives have been widely highlighted as anticancer, antimicrobial and anti-tumor agents. The polar β naphthol, soluble in water are found potentially less toxic to human.

In view of diverse biological and pharmacological applications of phenothiazines and β naphthol, they represent a good lead in developing and designing of virgin and new binary drugs. However, very little information is available with regard to binary drug materials of eutectic, non eutectic and additive types solid dispersions. In recent years pharmaceutical properties of some binary solid dispersion/co-crystals

Research Article

has been reported emphasizing the solubility, dissolution rate, hygroscopicity and chemical stability. Keeping the view of better pharmacological performance and efficacy of binary product, in this communication, it is aimed at investigating the phenothiazines (PT) and β naphthol (βN) binary drug dispersions in the solid state emphasizing thermodynamic and interfacial studies, such as phase diagram, excess and mixing thermodynamic functions, activity and activity coefficient, thermal stability, interfacial energy, surface roughness, driving force of solidification and critical radius.

Experimental Details

Phenothiazines (PT) (Sigma, India) and β naphthol (βN) were directly taken for investigation. The melting point of Phenothiazines was found 189°C while for β naphthol it was found 124°C. For measuring the solid-liquid equilibrium data of PT- βN system, mixtures of different compositions of both were made in glass test tubes by repeated heating and followed by chilling in ice and melting temperatures of solid dispersions were determined by the thaw-melt method (Salim, 2009). The melting and thaw temperatures were determined in a Toshniwal melting point apparatus using a precision thermometer which could read correctly up to ± 0.1°C. The heater was regulated to give above 1°C increase in temperature in every five minutes. The literature value (Singh *et al.,* 2014) of enthalpy of fusion of Phenothiazines and β naphthol was used in determining the various thermodynamic parameters of the binary system.

RESULTS AND DISCUSSION

SLE Study

The solid liquid equilibrium (SLE) data of PT-βN system determined by the thaw melt method is reported in Table 1. The system shows the formation of a eutectic (E) and non-eutectics solid dispersions (A1-A8). The melting point of PT (189°C) decreases on the addition of second component βN (M.P., 124°C) and further attains minimum and then increases. Eutectic E (0.237 mole fraction of PT) is obtained at 110°C. At the eutectic temperature a liquid phase L and two solid phases (S_1 and S_2) are in equilibrium and the system is invariant. The homogenous binary liquid solution exists in the region above the eutectic temperature while the two solid phases exists in the region below the eutectic temperature. The region located below the liquidus line on the left side a binary liquid and solid PT exist while in a similar region located on the right side a binary liquid and solid βN system co-exist.

$$L \xrightleftharpoons{\text{Cooling}} S_1 + S_2$$
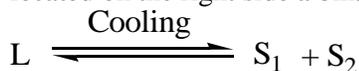
Thermodynamic Study

The values of heats of fusion of eutectic and non-eutectic are calculated by the mixture law. The value of heat of fusion of binary solid dispersions A_1-A_8 and E is reported in Table 1. The activity coefficient and activity of components for the systems under investigation has been calculated from the equation (Sharma *et al.,* 2009) given below

$$-\ln\chi_i\gamma_i = \frac{\Delta H_i}{R}\left(\frac{1}{T_e} - \frac{1}{T_i}\right)$$

(1)

where χ_i, γ_i is mole fraction and activity coefficient of the component *i* in the liquid phase respectively. ΔH_i is the heat of fusion of component i at its melting point T_i and R is the gas constant. T_e is the melting temperature of alloy. Using the values of activity and activity coefficient of the components in the binary product, the mixing and excess thermodynamic functions have been evaluated.

Mixing Functions

In order to know the mixing characteristics of components in the system Integral molar free energy of mixing (ΔG^M), molar entropy of mixing (ΔS^M) and molar enthalpy of mixing ΔH^M) and partial thermodynamic mixing functions of the binary solid dispersions were determined by using the following equations

Research Article

$$\Delta G^M = RT\,(\chi_{PT}\,\ln a_{PT} + \chi_{\beta N}\,\ln a_{\beta N}) \tag{2}$$

$$\Delta S^M = -R\,(\chi_{PT}\,\ln\chi_{PT} + \chi_{\beta N}\,\ln\chi_{\beta N}) \tag{3}$$

$$\Delta H^M = RT\,(\chi_{PT}\,\ln\gamma_{PT} + \chi_{\beta N}\,\ln\gamma_{\beta N}) \tag{4}$$

$$G_i^{-M} = \mu_i^{-M} = RT\,\ln a_i \tag{5}$$

where G_i^{-M} (μ_i^{-M}) is the partial molar free energy of mixing of component i (mixing chemical potential)in binary mix and γ_i and a_i is the activity coefficient and activity of component respectively. The negative value (Wisniak *et al.,* 1978) of molar free energy of mixing of alloys (Table 2) suggests that the mixing in all cases is spontaneous. The integral molar enthalpy of mixing value corresponds to the value of excess integral molar free energy of the system favors the regularity in the binary solutions.

Excess Functions
In order to unfold the nature of the interactions between the components forming the eutectic and non-eutectic solid dispersions, the excess thermodynamic functions such as integral excess integral free energy (g^E), excess integral entropy (s^E) and excess integral enthalpy (h^E) were calculated using the following equations

$$g^E = RT(\chi_{PT}\ln\gamma_{PT} + \chi_{\beta N}\ln\gamma_{\beta N}) \tag{6}$$

$$s^E = -R\left((\chi_{PT}\ln\gamma_{PT} + \chi_{\beta N}\ln\gamma_{\beta N} + \chi_{PT}T\frac{\delta\ln\gamma_{PT}}{\delta T} + \chi_{\beta N}T\frac{\delta\ln\gamma_{\beta N}}{\delta T} \right) \tag{7}$$

$$h^E = -RT^2\left(\chi_{PT}\frac{\delta\ln\gamma_{PT}}{\delta T} + \chi_{\beta N}\frac{\delta\ln\gamma_{\beta N}}{\delta T} \right) \tag{8}$$

and excess chemical potential or excess partial free energy of mixing;

$$g_i^{-E} = \mu_i^{-M} = RT\ln\gamma_i \tag{9}$$

The values of $\delta\ln\square_i/\delta T$ can be determined by the slope of liquidus curve near the alloys. The values of the excess thermodynamic functions are given in Table 3. The value of the excess free energy is a measure of the departure of the system from ideal behaviour. The reported excess thermodynamic data substantiate the earlier conclusion of an appreciable interaction between the parent components during the formation of alloys. The positive g^E value (Chen *et al.,* 2011, Nieto *et al.,* 1999) for all eutectic and non-eutectic solid dispersions infers stronger interaction between like molecules in binary mix. The excess entropy is a measure of the change in configurational energy due to a change in potential energy and indicates an increase in randomness.

Gibbs-Duhem Equation
Further the partial molar quantity, activity and activity coefficient can also be determined by using Gibbs-Duhem equation (Shekhar *et al.,* 2009)

$$\sum\chi_i dz_i^{-M} = 0 \tag{10}$$

$$or\ \ \chi_{PT}dH_{PT}^{-M} + \chi_{\beta N}dH_{\beta N}^{-M} = 0 \tag{11}$$

$$or\ \ dH_{PT}^{-M} = \frac{\chi_{\beta N}}{\chi_{PT}}dH_{\beta N}^{-M} \tag{12}$$

$$or\ \ [H_{PT}^{-M}]_{x_{PT}=y} = \int_{\chi_{PT}=y}^{\chi_{PT}=1}\frac{\chi_{\beta N}}{\chi_{PT}}dH_{\beta N}^{-M} \tag{13}$$

Research Article

Using equation (13) a graph between $H_{\beta N}^{-M}$ and $\chi_{\beta N}/\chi_{PT}$ gives the solution of the partial molar heat of mixing of a constituent PT in binary mix and plot between $\chi_{\beta N}/\chi_{PT}$ vs $\ln a_{\beta N}$ determines the value of activity of component PT in binary mix.

Stability Function

Thermodynamic behavior of the present system in form of stability and excess stability functions (Shekhar *et al.,* 2015) can be determined by the second derivative of their molar free energy and excess energy respectively, with respect to the mole fraction of either constituent:

$$\text{Stability} = \frac{\partial^2 \Delta G^M}{\partial x^2} = -2RT \frac{\partial \ln a}{\partial (1-x)^2} \tag{14}$$

$$\text{Excess Stability} = \frac{\partial^2 g^E}{\partial x^2} = -2RT \frac{\partial \ln \gamma}{\partial (1-x)^2} \tag{15}$$

These values were calculated by multiplying the slope of $\ln a$ vs $(1-x)^2$ and $\ln\gamma$ vs $(1-x)^2$ plots with -2RT. The best polynomial equation of the curve generated is given as:

$$\ln \gamma = 3.68(1-x)^2 - 21.44(1-x)^4 + 81.99(1-x)^6 - 146.84(1-x)^8 + 126.(1-x)^{10} - 41.47(1-x)^{12} \tag{16}$$

The slope of the curve shown in figure as obtained by differentiating the above equation with respect to $(1-x)^2$ may also be used to calculate the excess stability of the PT-βN system. The values of total stability to the ideal stability and defined as

$$\text{Ideal Stability} = \frac{RT}{x(1-x)} \tag{17}$$

These values show there is considerable thermodynamic stability in the alloy. The figure 4 for the stability, excess stability and ideal stability in the form of composition and partial Gibb's energy favours the formation of the binary alloys and their mixing.

Interfacial Investigation

The Solid-Liquid Interfacial Energy (σ)

It has been realized that an experimentally observed value of interfacial energy 'σ' keeps a variation of 50-100% from one worker to other. However, it was calculated the solid-liquid interfacial energy (σ) from melting enthalpy change (Bai *et al.,* 2006; Bayram *et al.,* 2013) and values obtained are found in good agreement with the experimental values. Turnbull empirical relationship between the interfacial energy and enthalpy change provides the clue to determine the interfacial energy value of binary solid dispersions and is expressed as:

$$\sigma = \frac{C\Delta H}{(N)^{1/3}(V_m)^{2/3}} \tag{18}$$

where the coefficient *C* lies between 0.33 to 0.35 for nonmetallic system, V_m is molar volume and N is the Avogadro's constant. The value of the solid-liquid interfacial energy of phenothiazine and β naphthol was found to be 3.61 x 10^{-02} and 3.70 x 10^{-02} J m^{-2} respectively and σ value of the solid dispersions was given in Table 1. The value of σ has also been determined by using the value of Gibbs-Thomson coefficient. The theoretical basis of determination of τ was made for equal thermal conductivities of solid and liquid phases for some transparent materials.

Gibbs-Thomson Coefficient (τ)

For a planar grain boundary on planar solid-liquid interface the Gibbs-Thomson coefficient (τ) for the system can be calculated by the Gibbs-Thomson equation and is expressed as

$$\tau = r\Delta T = \frac{TV_m\sigma}{\Delta H} = \frac{\sigma}{\Delta S_V} \tag{19}$$

where τ is the Gibbs-Thomson coefficient, ΔT is the dispersion in equilibrium temperature and, r is the radius of grooves of interface. It was also determined the numerical method (Shekhar *et al.,* 2013) for

Research Article

materials having known grain boundary shape, temperature gradient in solid and the ratio of thermal conductivity of the equilibrated liquid phases to solid phase ($R = K_L/K_S$). The Gibbs-Thomson coefficient for PT, βN and their solid dispersions are found in the range of $7.48 – 9.51 \times 10^{-06}$ Km and is reported in Table 1.

Interfacial Grain Boundary Energy (σ_{gb})
Grain boundary is the internal surface which can be understood in a very similar way to nucleation on surfaces in liquid-solid transformation. In past, a numerical method (Shekhar *et al.*, 2013) is applied to observe the interfacial grain boundary energy (σ_{gb}) without applying the temperature gradient for the grain boundary groove shape. For isotropic interface there is no difference in the value of interfacial tension and interfacial energy. A considerable force is employed at the grain boundary groove in anisotropic interface. The grain boundary energy can be obtained by the equation:

$$\sigma_{gb} = 2\sigma \cos \theta \tag{20}$$

where θ is equilibrium contact angle precipitates at solid-liquid interface of grain boundary. The grain boundary energy could be twice the solid-liquid interfacial energy in the case where the contact angle tends to zero. The value of σ_{gb} for solid PT and βN was found to be 6.98×10^{-2} and 7.15×10^{-2} Jm^{-2} respectively and the value for all solid dispersions is given in Table 1.

The Effective Entropy Change (ΔS_v)
It is obvious that the effective entropy change and the volume fraction of phases in the alloy are inter-related to decide the interface morphology during solidification and the volume fraction of the two phases depends on the ratio of effective entropy change of the phases. The entropy of fusion ($\Delta S = \Delta H/T$) value (Table 1) of alloys is calculated by heat of fusion values of the materials. The effective entropy change per unit volume (ΔS_V) is given by

$$\Delta S_V = \frac{\Delta H}{T} \cdot \frac{1}{V_m} \tag{21}$$

where ΔH is the enthalpy change, T is the melting temperature and V_m is the molar volume of solid phase. The entropy of fusion per unit volume (ΔS_V) for PT and βN was found 379.62 and 495.32 kJK^{-1}m^{-3} respectively. Values of ΔS_V for alloys are reported in Table 1.

The Driving Force of Nucleation (ΔG_v)
During growth of crystalline solid there is change in enthalpy, entropy and specific volume and non-equilibrium leads the Gibb's energy. Thermodynamically metastable phase occurs in a supersaturated or super-cooled liquid. The driving force for liquid-solid transition is the difference in Gibb's energy between the two phases. The theories of solidification process in past have been discussed on the basis of diffusion model, kinetic characteristics of nucleation and on thermodynamic features. The lateral motion of rudementry steps in liquid advances stepwise with non-uniform surface at low driving force while continuous and uniform surface advances at sufficiently high driving force. The driving force of nucleation from liquid to solid during solidification (ΔG_V) can be determined at different undercoolings (ΔT) by using the following equation

$$\Delta G_V = \Delta S_v \Delta T \tag{22}$$

It is opposed by the increase in surface free energy due to creation of a new solid-liquid interface. By assuming that solid phase nucleates as small spherical cluster of radius arising due to random motion of atoms within liquid. The value of ΔG_V for each solid dispersions and pure components are shown in the Table 4.

The Critical Radius (r*)
During liquid-solid transformation embryos are rapidly dispersed in unsaturated liquid and on undercooling liquid becomes saturated and provides embryo of a critical size with radius r* for nucleation which can be determined by the Chadwick relation (Chadwick, 1972)

$$r^* = \frac{2\sigma}{\Delta G_V} = \frac{2\sigma T}{\Delta H_V \Delta T} \tag{23}$$

Research Article

where σ is the interfacial energy and ΔH_v is the enthalpy of fusion of the compound per unit volume, respectively. The critical size of the nucleus for the components and alloys was calculated at different undercoolings and values are presented in Table 5. It can be inferred from table that the size of the critical nucleus decreases with increase in the undercooling of the melt. The existence of embryo and a range of embryo size can be expected in the liquid at any temperature. The value of r* for pure components (PT and βN) and solid dispersions lies between 43 to 191 nm at undercooling 1 – 3.5°C.

Critical Free Energy of Nucleation (ΔG*)

To form critical nucleus, it requires a localized activation/critical free energy of nucleation (ΔG*) which is evaluated as

$$\Delta G^* = \frac{16}{3} \frac{\pi \sigma^3}{\Delta G_v^2}$$

(24)

The value of ΔG* for alloys and pure components has been found in the range of 10^{-15} to 10^{-16} J per molecule at different undercoolings, and has been reported in Table 6.

Interface Morphology

The science of growth has been developed on the foundation of thermodynamics, kinetics, fluid dynamics, crystal structures and interfacial sciences. The solid-liquid interface morphology can be predicted from the value of the entropy of fusion. According to Hunt *et al.,* (1994) the type of growth from a binary melt depends upon a factor α, defined as:

$$\alpha = \xi \frac{\Delta H}{RT} = \xi \frac{\Delta S}{R}$$

(25)

where ξ is a crystallographic factor depending upon the geometry of the molecules and has a value less than or equal to one. ΔS/R (also known as Jackson's roughness parameter α) is the entropy of fusion (dimensionless) and R is the gas constant. When α is less than two the solid-liquid interface is atomically rough and exhibits non-faceted growth. The value of Jackson's roughness parameter (α) is given in Table 1. For the entire solid dispersions the α value was found greater than 2 which indicate the faceted (Bergeon *et al.,* 2005, Shekhar *et al.,* 2011) growth proceeds in all the cases.
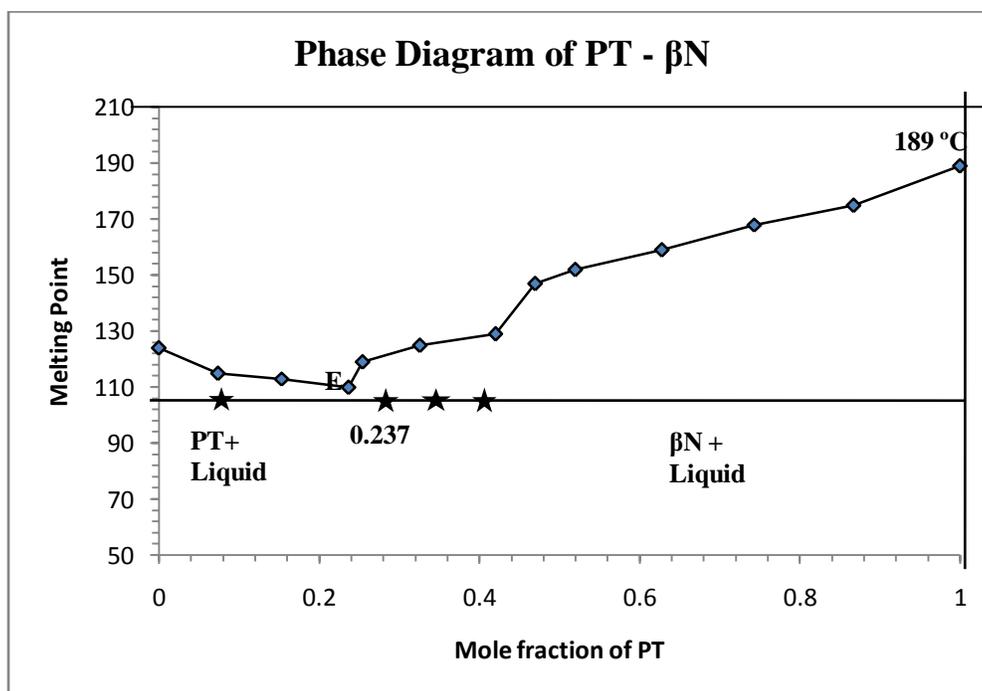
Figure No and Title Missing

Research Article
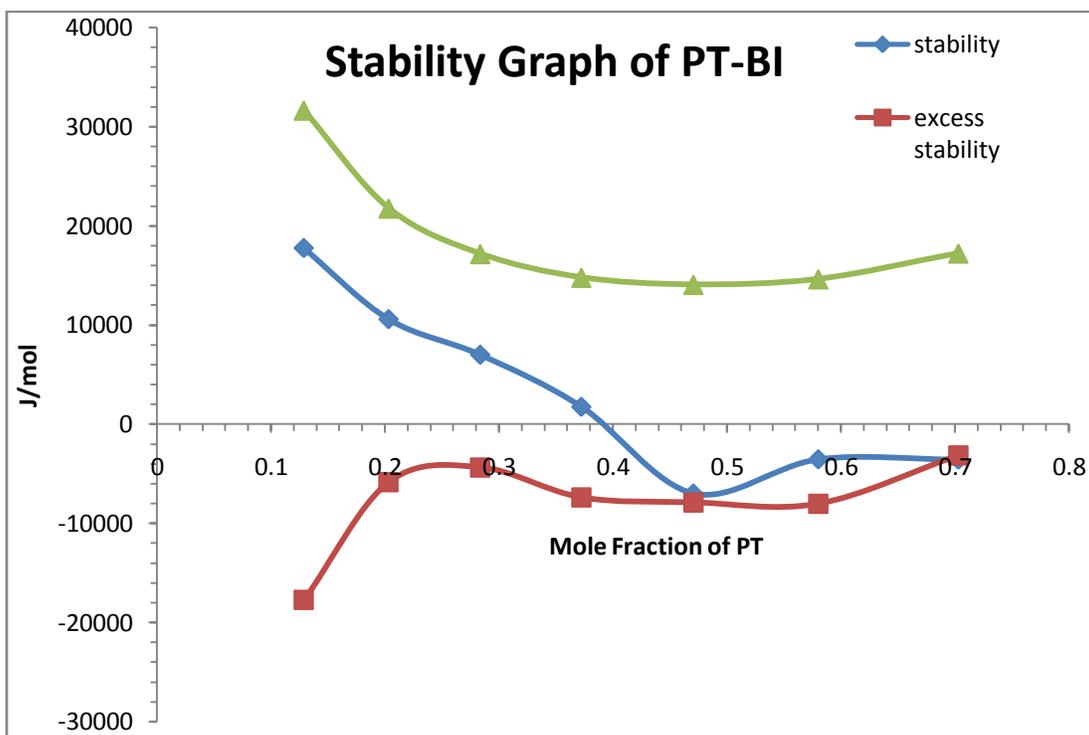
Figure No and Title Missing

Table 1: Phase composition, melting temperature, values of entropy of fusion per unit volume (ΔS_v), heat of fusion(ΔH), interfacial energy(σ), grain boundary energy(σ_{gb}), Gibbs-Thomson coefficient (τ) and roughness parameter(α)

Alloy	χ_{PT}	MP	ΔH(J/mol)	ΔS (J/mol/K)	α	σ x 10^2 (J/m²)	σ_{gb} × 10^2 (J/m²)	ΔS_v (kJ/m³/K)	ΔH_v	τ × 10^6 Km
A1	0.074	115	22289.36	57.45	6.91	3.69	7.13	501.63	194.63	7.36
A2	0.153	113	22576.92	58.49	7.04	3.68	7.12	498.92	192.58	7.38
E	0.237	110	22882.68	59.75	7.19	3.67	7.10	497.40	190.51	7.38
A3	0.254	119	22944.53	58.53	7.04	3.67	7.09	484.94	190.10	7.57
A4	0.326	125	23206.64	58.31	7.01	3.66	7.08	473.39	188.41	7.74
A5	0.420	129	23548.80	58.58	7.05	3.65	7.06	463.45	186.31	7.88
A6	0.469	147	23728.21	56.50	6.80	3.65	7.05	441.07	185.25	8.27
A7	0.520	152	23912.80	56.27	6.77	3.64	7.04	433.38	184.19	8.41
A8	0.628	159	24305.92	56.26	6.77	3.64	7.02	421.33	182.02	8.63
A9	0.743	168	24724.52	56.06	6.74	3.63	7.01	407.79	179.83	8.89
A10	0.867	175	25175.88	56.20	6.76	3.62	6.99	396.47	177.62	9.13
PHZ		189	25660.00	55.54	6.68	3.61	6.98	379.62	175.38	9.51
βN		124	22020.00	55.47	6.67	3.70	7.15	495.32	196.64	7.48

Research Article

Table 2: Value of partial and integral mixing of Gibbs free energy(ΔG^M), enthalpy(ΔH^M) and entropy(ΔS^M) of PT – βN system

Alloy	$\Delta G_{PT}{}^{-M}$ J/mol	$\Delta G_{\beta N}{}^{-M}$ J/mol	ΔG^M J/mol	$\Delta H_{PT}{}^{-M}$ J/mol	$\Delta H_{\beta N}{}^{-M}$ J/mol	ΔH^M J/mol	$\Delta S_{PT}{}^{-M}$ J/mol/K	$\Delta S_{\beta N}{}^{-M}$ J/mol/K	ΔS^M J/mol/K
A1	-4110.04	-499.19	-766.40	4289.02	-251.19	84.79	21.65	0.64	2.19
A2	-4221.13	-610.13	-1162.61	1803.57	-77.22	210.54	15.61	1.38	3.56
E	-4387.75	-776.52	-1632.38	196.62	84.81	111.31	11.97	2.25	4.55
A3	-3887.88	-277.33	-1194.38	578.56	677.64	652.47	11.39	2.44	4.71
A4	-3554.63	55.47	-1121.43	154.26	1360.94	967.56	9.32	3.28	5.25
A5	-3332.47	277.33	-1238.78	-433.08	2097.93	1034.91	7.21	4.53	5.66
A6	-2332.73	1275.72	-417.69	309.00	3487.96	1996.11	6.29	5.27	5.75
A7	-2055.02	1553.05	-323.15	255.59	4146.49	2123.23	5.44	6.10	5.76
A8	-1666.23	1941.31	-324.23	4.66	5492.95	2046.30	3.87	8.22	5.49
A9	-1166.36	2440.50	-239.40	-77.20	7422.07	1850.11	2.47	11.30	4.74
A10	-777.58	2828.77	-297.93	-246.00	10342.94	1162.33	1.19	16.77	3.26

Table 3: Value of partial and integral excess Gibbs free energy(g^E), enthalpy(h^E) and entropy(s^E) of PT - βN system

Alloy	$g_{PT}{}^{-E}$ J/mol	$g_{\beta N}{}^{-E}$ J/mol	g^E J/mol	$h_{PT}{}^{-E}$ J/mol	$h_{\beta N}{}^{-E}$ J/mol	h^E J/mol	$s_{PT}{}^{-E}$ J/mol/K	$s_{\beta N}{}^{-E}$ J/mol/K	s^E J/mol/K
A1	4289.02	-251.19	84.79	143478.22	-8503.55	2743.10	358.74	-21.27	6.85
A2	1803.57	-77.22	210.54	217232.69	21855.54	51748.24	558.11	56.82	133.52
E	196.62	84.81	111.31	38663.44	-2040.11	7606.63	100.44	-5.55	19.57
A3	578.56	677.64	652.47	12064.65	-9176.03	-3781.09	29.30	-25.14	-11.31
A4	154.26	1360.94	967.56	55135.76	17059.25	29472.19	138.14	39.44	71.62
A5	-433.08	2097.93	1034.91	-9665.05	-10437.45	-10113.04	-22.97	-31.18	-27.73
A6	309.00	3487.96	1996.11	-10034.36	-8202.77	-9062.32	-24.63	-27.84	-26.33
A7	255.59	4146.49	2123.23	3219.16	9265.76	6121.53	6.97	12.05	9.41
A8	4.66	5492.95	2046.30	-953.12	19689.46	6725.92	-2.22	32.86	10.83
A9	-77.20	7422.07	1850.11	1542.47	56623.73	15698.36	3.67	111.57	31.40
A10	-246.00	10342.94	1162.33	-62.44	144845.31	19210.29	0.41	300.23	40.29

Research Article

Table 4: Value of volume free energy change (ΔG_v) during solidification for PT - βN system of different undercoolings (ΔT)

Alloy	ΔG_v(J/cm^3)					
	1.0	1.5	2.0	2.5	3.0	3.5
A1	0.50	0.75	1.00	1.25	1.50	1.76
A2	0.50	0.75	1.00	1.25	1.50	1.75
E	0.50	0.75	0.99	1.24	1.49	1.74
A3	0.48	0.73	0.97	1.21	1.45	1.70
A4	0.47	0.71	0.95	1.18	1.42	1.66
A5	0.46	0.70	0.93	1.16	1.39	1.62
A6	0.44	0.66	0.88	1.10	1.32	1.54
A7	0.43	0.65	0.87	1.08	1.30	1.52
A8	0.42	0.63	0.84	1.05	1.26	1.47
A9	0.41	0.61	0.82	1.02	1.22	1.43
A10	0.40	0.59	0.79	0.99	1.19	1.39
PHZ	0.38	0.57	0.76	0.95	1.14	1.33
βN	0.50	0.74	0.99	1.24	1.49	1.73

Table 5: Critical size of nucleus (r*) at different undercoolings (ΔT)

Alloy	r*(nm)					
	1.0	1.5	2.0	2.5	3.0	3.5
A1	147.25	98.17	73.63	58.90	49.08	42.07
A2	147.64	98.43	73.82	59.06	49.21	42.18
E	147.69	98.46	73.84	59.07	49.23	42.20
A3	151.40	100.93	75.70	60.56	50.47	43.26
A4	154.76	103.17	77.38	61.90	51.59	44.22
A5	157.67	105.11	78.83	63.07	52.56	45.05
A6	165.46	110.31	82.73	66.18	55.15	47.27
A7	168.18	112.12	84.09	67.27	56.06	48.05
A8	172.57	115.04	86.28	69.03	57.52	49.30
A9	177.88	118.59	88.94	71.15	59.29	50.82
A10	182.55	121.70	91.28	73.02	60.85	52.16
PHZ	190.26	126.84	95.13	76.10	63.42	54.36
βN	149.55	99.70	74.77	59.82	49.85	42.73

Research Article

Table 6: Value of critical free energy of nucleation (ΔG*) for alloys of PT - βN system at different undercooling (ΔT)

Alloy	$\Delta G^* \times 10^{16}$ (J)					
	1.0	1.5	2.0	2.5	3.0	3.5
A1	33.56	14.92	8.39	5.370	3.730	2.740
A2	33.64	14.95	8.41	5.380	3.740	2.750
E	33.57	14.92	8.39	5.370	3.730	2.740
A3	35.26	15.67	8.82	5.640	3.920	2.880
A4	36.76	16.34	9.19	5.880	4.080	3.000
A5	38.06	16.92	9.52	6.090	4.230	3.110
A6	41.86	18.61	10.47	6.700	4.650	3.420
A7	43.20	19.20	10.80	6.910	4.800	3.530
A8	45.37	20.16	11.34	7.260	5.040	3.700
A9	48.09	21.37	12.02	7.690	5.340	3.930
A10	50.54	22.46	12.63	8.090	5.620	4.130
PHZ	54.78	24.35	13.69	8.760	6.090	4.470
βN	34.71	15.43	8.68	5.550	3.860	2.830

Conclusion
The solid-liquid equilibrium phase diagram of PT-βN system shows the formation of simple eutectic alloy. The activity and activity coefficient values are very useful in computing thermodynamic mixing and excess functions. Thermodynamic excess and mixing functions g^E and ΔG^M values for eutectic and non-eutectics are being found positive which suggest the stronger association between like molecules and there is non-spontaneous mixing in all the binary drugs.

REFERENCES
Attila Bende, Ion Grosu and Ion Turcu (2010). Molecular modeling of Phenothiazine derivatives: Self-Assembling properties, *The Journal of Physical Chemistry A* **114** 12479-12489.
Bai Xian-Ming and Li Mo (2006). Calculation of Solid-liquid interfacial free energy: A classical nucleation theory based approach. *The Journal of Chemical Physics* **124** 124707-12.
Bayram Ü, Aksöz S and Maraşlı N (2013). Solid–liquid interfacial energy of solid aminomethylpropanediol solution in equilibrium with aminomethylpropanediol – neopentylglycol – D camphor liquid. *Thermochimica Acta* **554** 48-53.
Bergeon N, Trivedi R, Billia B, Echebarria B, Karma A, Liu S, Weiss C and Mangelinck N (2005). Necessity of investigating microstructure formation during directional solidification of transparent alloys in 3D. *Advances in Space Research* **36** 80-85.
Chadwick GA (1972). *Metallography of Phase Transformation* (Butterworths, London) 61.
Chen Bin-Yuan, Zhang Xue-Sheng and Li Ding-Long (2011). Theoretical study on Thermodynamic Properties and Hydrophilicity of Polychlorinated Phenothiazines. *Chinese Journal of Structural Chemistry* **30**(11) 1575-1584.
Domínguez JN, López S, Charris J, Iarruso L, Lobo G, Semenov A, Olson JE and Rosenthal PJ (1997). Synthesis and antimalarial effects of phenothiazine inhibitors of a Plasmodium falciparum cysteine protease. *Journal of Medicinal Chemistry* **40** 2726-2732.
Guerrero-Martínez A, Montoro T and Viñas MH (2008). Tardajos G,Complexation and Chiral Drug Recognition of an Amphiphilic Phenothiazine Derivative with β-Cyclodextrin. *Journal of Pharmaceutical Sciences* **97** 1485-1498.

Research Article

Gupta P, Agrawal T, Das SS and Singh NB (2011). Solvent Free Reactions, Reactions of Nitrophenols in 8-Hydroxyquinoline-Benzoic Acid Eutectic Melt. *Journal of Thermal Analysis and Calorimetry* **104**(3) 1167-1176.

Hunt JD and Lu SZ (1994). *Hand Book of Crystal Growth,* edited by Hurle DTJ (Elsevier, Amsterdam) 112.

Nieto R, Gonzalez MC and Herrero F (1999). Thermodynamics of mixtures, Function of mixing and excess functions. *American Journal of Physics* **67** 1096-1099.

Salim SS (2009). Study of Multiphase Organic Materials. Ph. D. Thesis, V. K. S. University, Ara, Bihar.

Sharma BL, Tandon S and Gupta S (2009). Characteristics of the binary faceted eutectic: benzoic acid –salicylic acid system, *Crystal Research and Technology* **44**(3) 258 – 268.

Shekhar H and Kant Vishnu (2011). Kinetic and Interfacial Studies on Transparent Organic Alloys. *Journal of the Indian Chemical Society* **88** 947-952.

Shekhar H and Kant Vishnu (2013). *Thermodynamics of Nicotinamide Based Binary Drug System* (Lambert Academic publishing Germany).

Shekhar H and Kumar Manoj (2015). Thermodynamic and Interfacial Investigation of Phenothiazine-Resorcinol Binary System. *International Journal of Chemistry* **4**(3) 268-277.

Shekhar H and Kumar Manoj (2015). Thermodynamic and interfacial studies on solid dispersions of phenothiazine-2-methylimidazole drug system. *Journal of Chemical and Pharmaceutical Research* **7**(1) 37-45.

Shekhar H, Salim SS and Kumar N (2009). Thermodynamic Investigation of alloys of Phenanthrene-Benzidine System. *Journal of International Academy of Physical Sciences* **13** 473-150.

Singh Jayram, Rai Sarita and Singh NB (2014). Phase Equilibria and Crystallization Behaviour of Succinonitrile - 8-Hydroxyquinoline Eutectic System. *JSM Chemistry* **2** 1010.

Wisniak J and Tamir A (1978). *Mixing and Excess Thermodynamic Properties* (a literature source book) (Phys. Sci. Data 1, Elsevier, New York).

Yu L and Reutzel-Edens SM (2003). *Crystallization, Encyclopedia of Food Sciences and Nutrition,* second edition (Elsivier Science Ltd. Amsterdam).